Network for Research and Development in Africa
International Journal of Pure and Applied Science Research
ISSN: 2384-5918. Volume 13, Number 1
Pages 22-35 (February, 2023)
DOI: 45727711312
www.arcnjournals.org

Effect of OPEFB Filler on the Magnitudes of Transmission and Reflection Coefficient of OPEFB-HDPE Composite at Microwave Frequency

Charles Suleiman Bwala[1], Sunday Dauda Balami[2], [3]Mustapha Aliyu
[1,2]Department of Science Laboratory Technology, Ramat Polytechnic Maiduguri, Nigeria

Abstract: *The transmission/reflection properties of high-density polyethylene (HDPE) filled with oil palm empty fruit bunch (OPEFB) have been investigated at filler loadings, 30, 50, and 70 percent. The OPEFB-HDPE composites were prepared using the conventional melt blend method. The T/R coefficients were measured using PNA-L (N5227A) Network Analyzer from 8 GHz to 12 GHz at room temperature, whereas the theoretical calculation of the T/R and visualization of electric field distribution of the sample placed in the waveguide was computed using FEM accomplished by COMSOL software. Due to high permittivity associated with OPEFB, the result showed that higher the HDPE content in the composites the lower is the permittivity. This led to higher values of the magnitude of the reflection coefficient $|S_{11}|$ and lower transmission coefficient $|S_{21}|$ by the impedance matching theory. Comparison of the measured and calculated scattering parameters as investigated were in agreement with each other. Furthermore, the electric field's distribution through the waveguide as visualized using FEM simulation revealed that the attenuation decreased as the OPEFB filler content is reduced.*

Keywords: *Attenuation, Simulation, Transmission Coefficient.*

1. INTRODUCTION

Information on materials conduct in an electromagnetic field is of enormous significance particularly when it identifies with military equipment, hardware, communication, and modern applications. The estimation of T/R coefficient of materials in the microwave frequency range is found in various areas. A good understanding of T/R measurement of these materials and its attenuation is necessary to get valuable knowledge from materials proposed for use in microwave absorption. Numerous methods have been used by various researchers over the years to calculate the T/R coefficient of samples at microwave frequency [1, 2]. Dudek et al and Kumar et al have used the vector network analyzer (VNA) successfully to obtain the S parameters of samples in the microwave wave range [3, 4]. Transmission/Reflection line

method is a popular broadband measurement method where it is assumed that only the fundamental waveguide mode (TEM mode in coaxial line and TE mode in waveguides) is propagated. The transmission and reflection line technique includes setting a sample in a segment of waveguide or coaxial line and measuring the two ports complex scattering parameters with a vector analyzer (PNA-L). For measurement to be done utilizing PNA-L, calibration must be completed. The technique includes estimation of the reflected (S_{11}) and transmitted flag (S_{21}). The applicable s-parameters relate nearly to the complex permittivity and permeability of the material [5, 6]. The transmission and reflection coefficients of the OPEFB-HDPE composite of various filler content and types of host matrix and material properties were not analyzed in details theoretically and experimentally.

FEM has since become a very useful tool in computational electromagnetic (CEM) with the development of vector elements and boundary integral equations to deal with open region scattering problems [7]. This method was used to validate S parameter measurement of PTFE and inorganic samples. Barkanov, [8] in his work stated that the three basic FEM procedures are formulation of the problem, discretization of the formulation and solution for the resulting finite element equations. FEM can be categorized into three electromagnetic domains, namely the electric intensity E, magnetic intensity H, and potential V. In solving the potential V domain, the scalar or vector finite element routines may be used. Whereas solving of electric intensity, E and magnetic intensity, H domains are effectively solved using vector finite element routine. Scalar routine cases are readily and easily obtained than vector routine. However, many electromagnetic problem reduction of unknown quantity to scalar potential is completely impossible. The solution to it is to find a two or three component vector field. FEM has the flexibility to solve many engineering problems delving down to microwave heating and high power transmitter design.

This work reported on the investigation of OPEFB fibre as filler in compounding a high density polyethylene as host material. The fundamental objectives are to:

i. Determine the effect of OPEFB-HDPE composite ratio on the magnitudes transmission and reflection coefficient at 8 – 12 GHz microwave frequency.
ii. Compare the measured and simulated S-parameters obtained from rectangular waveguide via vector Network analyzer and finite element methods (FEM) respectively.
iii. Visualize the electromagnetic field distribution in the waveguide loaded with OPEFB-HDPE composites using finite element method (FEM).

Further, aside from the works cited above, OPEFB as filler in polymer materials has been reported in several literatures. Thus, it has been employed as filler in the production of the composites such as: polypropylene [18, 19], poly(vinyl chloride) [20], polyurethane [21, 22], unsaturated polyester resin [23]. OPEFB has also been used in the production of polyethylene

composites [17, 24]. In all the above works mentioned, none investigated the effects of OPEFB-HDPE composites ratio on S-parameters at microwave frequency.

In this study, TE_{10} was utilized as the proliferating mode through the rectangular waveguide. Both in and out mode of the wave are given from an Eigen mode investigation on the waveguide cross section. The model employ the utilization of RF Module's Port boundary condition for resolving propagation of wave [16]. The scattering parameters is computed as a function of the dielectric constant automatically by the software. The attenuation of the OPEFB-HDPE in decibel (dB) was calculated from maximum electric field intensity inside the rectangular waveguide at ports where the wave enters and exits the waveguide.

2. METHODOLOGY

2.1. Experimental

All the data reported in this study were measured out at room temperature. Three different OPEFB-HDPE composites were made using various % of OPEFB as filler. The samples were named 30% PE, 50% PE and 70% PE. The 100% PE was however used as reference sample. The OPEFB-HDPE composites were prepared via the melt blend technique using the Brabender poly-drive three-phase motor with a drive of 1.5 kW, 3 x 230 V, 40 A and speed range of 0-120 rpm. For the purpose of this work, composites with dimensions of 0.22 cm x 0.11 cm x 0.006 cm were fabricated using a hydraulic press machine at 4 tones.

An Agilent N5227A PNA-L network analyzer setup in Fig. 1 was used to measure the S parameters of the cell containing the material under test over a range of frequencies (8 GHz-12 GHz). In this (TR) method the fundamental transverse electromagnetic TEM mode is the only mode that propagates in transmission line. For the correction and handling of all errors within the measurement, a full port calibration is best considered [15].

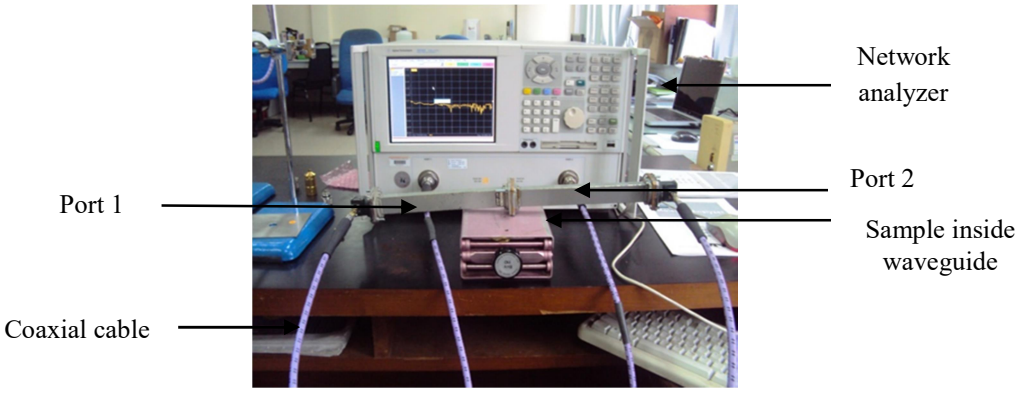

Fig. 1: T/R measurement using a PNA-L set-up

2.2. Finite Element Method

The wave equation for the waveguide is:

$$\nabla \times (\mu_r^{-1} \nabla \times E) - k_0^2 \left(\varepsilon_r - \frac{j\sigma}{\omega \tau_0}\right) E = 0 \qquad (1)$$

Where μ_r signifies the relative permeability, and k_0 the free space wave number, j the imaginary unit, σ the conductivity, ω the angular frequency, ε_r the relative permittivity, and ε_0 the permittivity of free space [16].

Because of the adaptability to fit into many shapes, the element chosen to discretize the waveguide space is a tetrahedron, shown in Fig. 2.

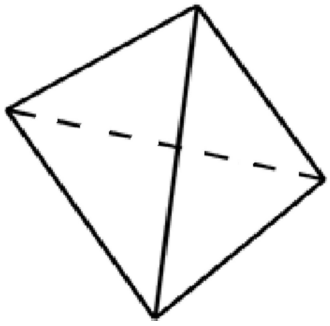

Fig 2: Tetrahedron element

As an initial step the Cross-area of the waveguides is drawn in two dimensions, with the material composite attuned. At that point a mesh comprising of triangles is created. The quantity of triangles increments with the electrical density of the material under test. The two dimensional mesh is extruded into depth with a limited number of layers, generating triangular-prism constituents or elements which thus hatchet parceled into tetrahedral. Thusly the three-dimensional waveguide is produced. Mesh of the waveguide with material sample inside is as shown in Fig. 3.

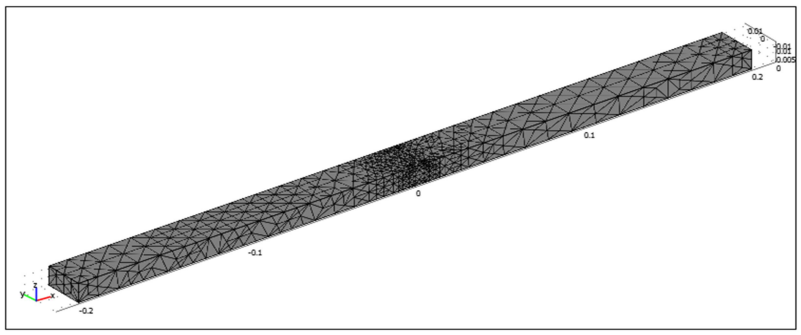

Fig. 3: Waveguide with generated sample mesh

Inside every tetrahedron the obscure field can be added from every node value by utilizing the first order polynomial. With this definition of the basis (interpolation), the electric field inside a lone Tetrahedron can be represented as

$$E^6 = \sum_{i=1}^{6} N_i^e E_i^e(x, y, z) \qquad (2)$$

Where, N_i^e =1, 2, 3...6 are the six complex amplitudes of electric field associated with the six edges of the tetrahedron, and $E_i^e(x, y, z)$ is the vector basis function associated with the ith edge of the tetrahedron. Detail derivation for the expression for E^e is given in reference [9]. Using equation (2) in boundary condition and integration over the volume of one tetrahedron then matrix form can be written for tetrahedron [10].

$$[S_e] \cdot [N^e] = [V] \qquad (3)$$

That V can be founded from boundary condition. These element matrices can be assembled over all the tetrahedron elements in region consist of sample to obtain a global matrix equation

$$[S] \cdot [N^e] = [V] \qquad (4)$$

The solution vector $[N^e]$ of the matrix equation (4) is then used to determine reflection and transmission coefficient. This study is based on both FEM simulation and experimental measurements.

3. RESULTS AND DISCUSSION

3.1. The effects of OPEFB-HDPE composite ratio on S_{11} and S_{21} magnitudes (RWG)

Figures 4 and 5 present the variation in S_{21} and S_{11} with respect to frequency respectively. Evidently from the result, the ripples nature of the $|S_{11}|$ and $|S_{21}|$ could be due to the internal surface roughness of the rectangular waveguide, air gab between the samples and the internal walls of the rectangular waveguide, sample imperfections and voids within the sample and the ripple nature is due to half wavelength effects and might also be attributed to the impedance mismatched between input impedance of the waveguide, the surface impedance of the sample and the characteristics impedance of the coaxial cable [11]. The result reveals multiple reflection for both S_{21} and S_{11}. This effect is attributed to the sample thickness being relatively small about 6 mm. However, if samples are sufficiently thick, there will be no multiple reflection and S_{21} will decrease with frequency [12]. The spikes or half wavelength effect in the graph is repeated every λ/2 due to multiple reflection effect in the sample [13].
Table 1 list the magnitudes of S_{21} and S_{11} for all composites at 8 GHz and 12 GHz. The result reveals that the higher the HDPE the higher the S_{21}, whist the higher the HDPE the lower the S_{11}. This is attributed to increase in loss factor as the % HDPE is decreased and the % OPEFB filler increased. The higher the Ɛ", the higher is the reflection and lower transmission is observed as the % of OPEFB filler is increased.

Table 1: Magnitudes of S_{21} and S_{11} at 8 GHz and 12 GHz

HDPE (%)	S_{21}		S_{11}	
	8 GHz	12 GHz	8 GHz	12 GHz
30	0.5066	0.7876	0.7966	0.3905
50	0.5913	0.7943	0.7098	0.4684
70	0.6778	0.8786	0.6102	0.3705
100	0.7385	0.9126	0.5764	0.3433

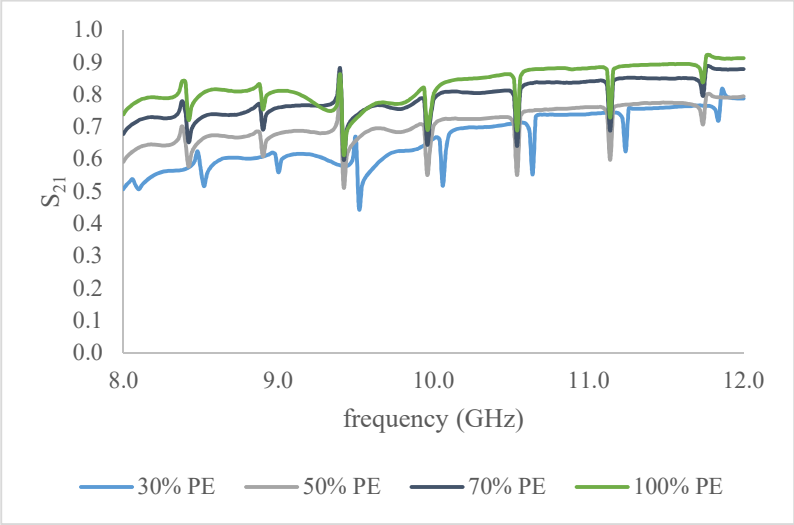

Fig. 4: Variation in S_{21} with frequency

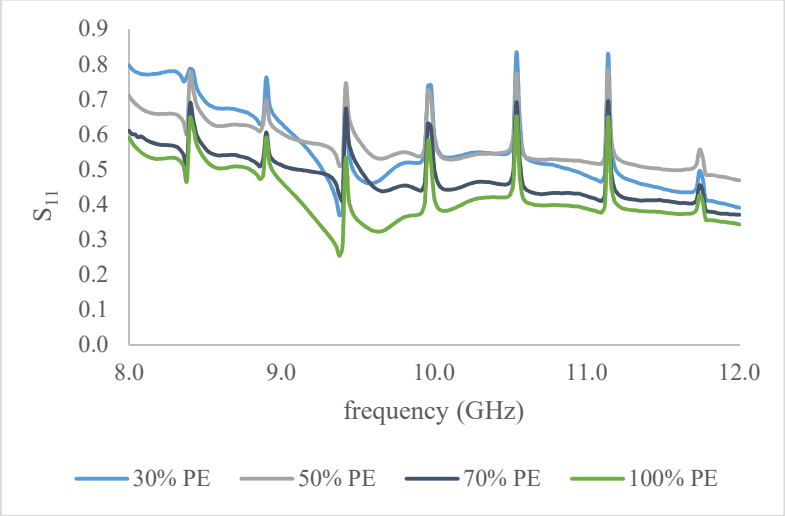

Fig. 5: Variation in S_{11} with frequency

3.2. Comparison of measured and simulated scattering parameters

The dielectric properties obtained from the rectangular waveguide method were used as initial input in FEM to calculate the $|S_{11}|$ and $|S_{21}|$ of the samples. The graphs in Fig. 6 and 7 are the

comparison between the measured and simulated (FEM) values of the $|S_{21}|$ and $|S_{11}|$ OPEFB-HDPE composites respectively. In general, the magnitude of $|S_{21}|$ increased with decreasing % OPEFB filler content, where the 70% PE sample was found to have the highest $|S_{21}|$ with corresponding lowest $|S_{11}|$. The change in $|S_{21}|$ and $|S_{11}|$ with frequency are proportional and inversely proportional respectively. The results are in agreement with each other. Tabulated in table 2 is the relative errors analysis of the rectangular waveguide with respect to simulated results calculated for S_{21}. Based on the analysis, the FEM has confirmed the measurement results. The relative errors are in the range between 0.0748 and 0.0519, far less than 1.

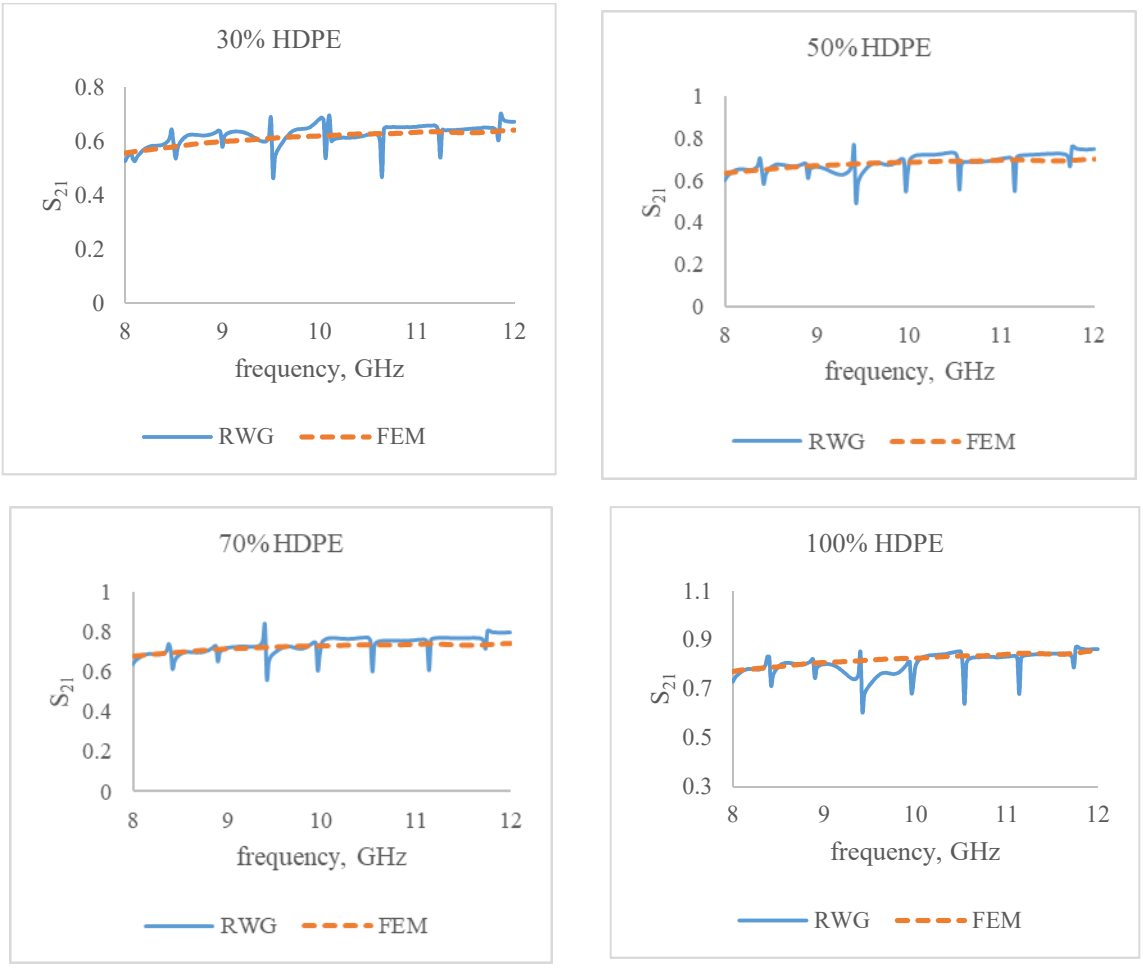

Fig. 6: Measured and simulated S_{21} for all samples

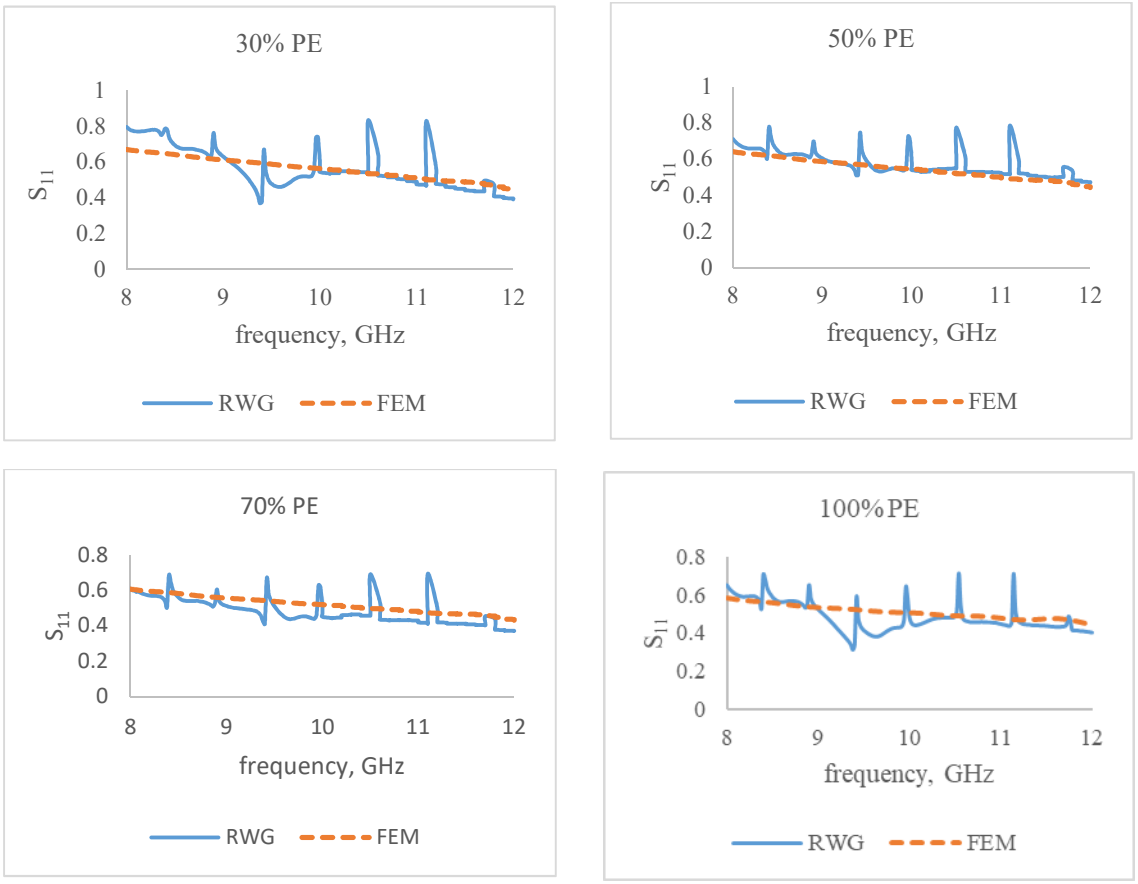

Fig. 7: Measured and simulated S_{11} for all samples

Table 2: Relative error of FEM with respect to RWG (S_{21})

Samples (% PE)	S_{21}		Relative error
	RWG	FEM	
30	0.6298	0.6128	0.0186
50	0.6823	0.6796	0.0039
70	0.7342	0.7215	0.0176
100	0.7912	0.8217	0.0212

3.3. Electric field z component in a waveguide

Figures 8(a) and (b) respectively showed FEM simulation for electric intensity in 2 dimension and 3 dimension surface plots for the 6 mm thick HDPE sample. The plots showed the variation of z-segment of the electrical field against the length of the rectangular waveguide. The x-axis represent the length of rectangular waveguide from - 0.2 to 0.2 m, whereas the z-axis is the electric field z component [14].

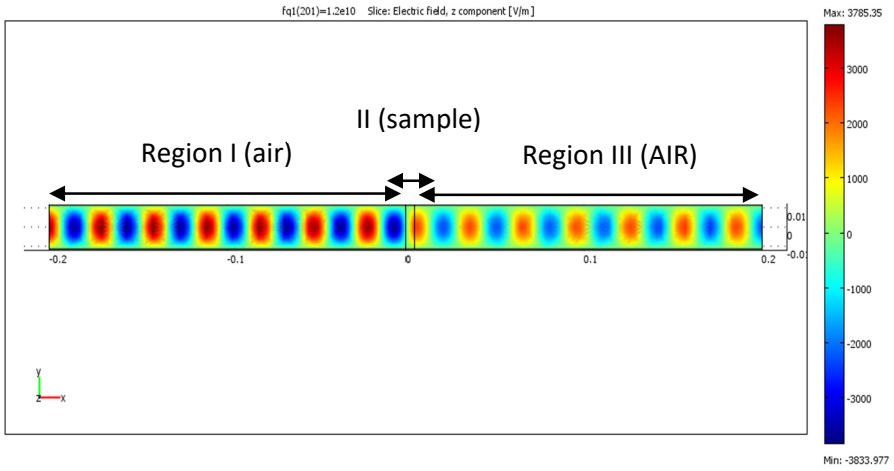

(a)

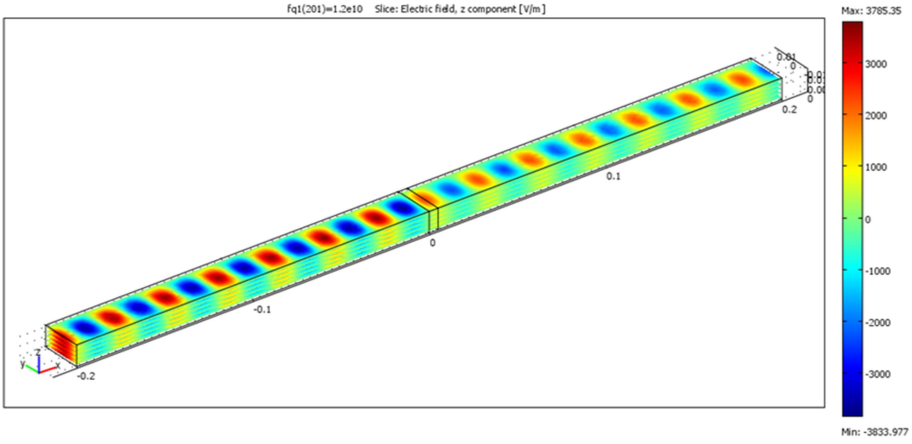

(b)

Fig. 8: Electric fields FEM simulation for 6 mm thick HDPE in (a) 2D (b) 3D surface plots

Attenuation is a function which can be affected by several factors. One factor affecting attenuation with regards to this work is the % of filler present in the composites. The % of OPEFB has influence on the transmission coefficient (S_{21}) as can be seen previously in Fig. 4. This in turn affect the intensity of attenuation coefficients of materials. Attenuation of OPEFB-HDPE a different OPEFB composition and 6 mm thicknesses is calculated in this work. The formula used to calculate attenuation for calculated FEM result is given as; [14]

$$Attenuation\ (dB) = -20log_{10}\left(\frac{maximum\ transmitted\ intensity}{maximum\ incident\ intensity}\right) \qquad (5)$$

In region I from -0.2 to 0.0, the maximum amplitude electric fields obtained was about 3979 V/m. As the wave was propagated through the material, the amplitude of the fields shrunk to 2230 V/m, i.e. only about 0.359 % of one wavelength of the propagated wave is in region II due to 6 mm thick sample. Therefore, the attenuation coefficient for 30% HDPE, of thickness 6 mm at 8 GHz frequency was calculated to be 5.72 dB due to the maximum amplitude of fields entering from region I and then exiting through region III of the rectangular waveguide. The corresponding attenuations for the 50% and 70% PE samples are 5.15 dB and 4.75 dB respectively. The trend showed a decreased attenuation as the % OPEFB filler content in the sample decreases. This is due to absorption from the cellulose present in the OPEFB.

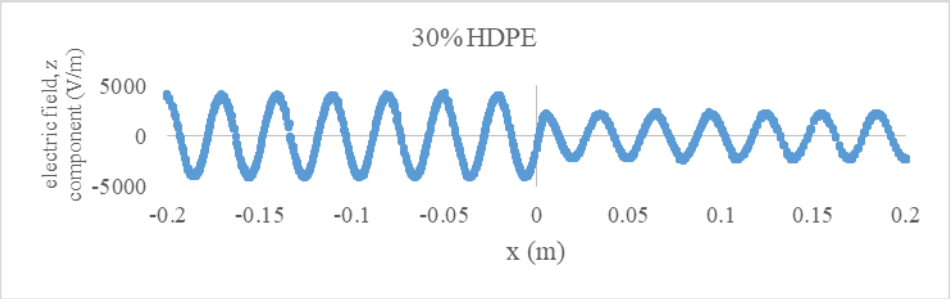

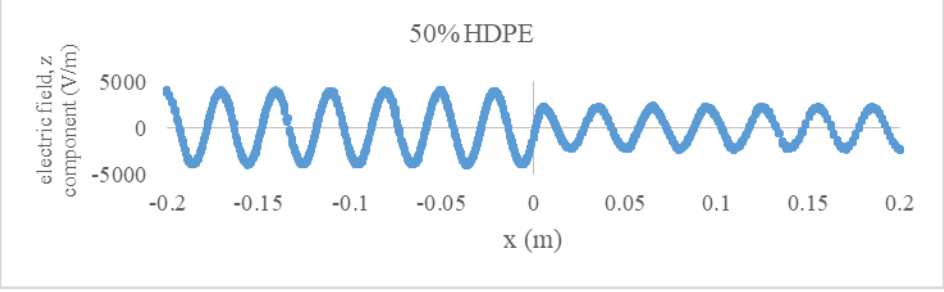

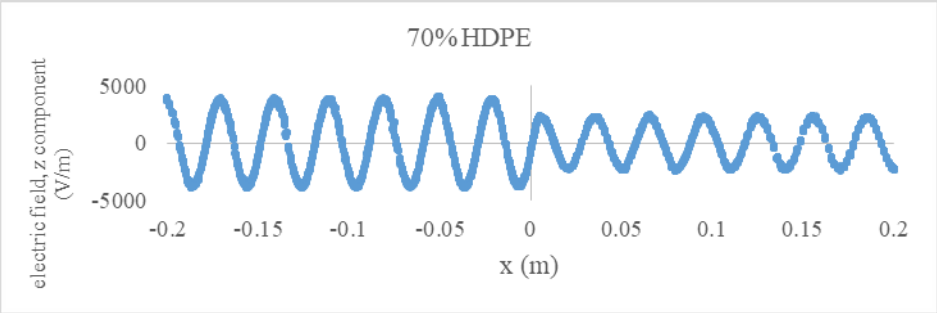

Fig. 9: Electric fields z component inside waveguide

Conclusion

The effect of the different % of OPEFB filler on the scattering parameters were investigated. The higher operating frequencies were found to give lower values of the amplitude of the reflection coefficients. Comparative analysis was carried out between measured and calculated scattering parameters using PNA-L and finite element method (FEM) respectively for samples placed on inside rectangular waveguide. The simulated result from FEM was found to predict correctly the measured results. FEM simulation was used to visualize the electric field distribution in the form of waves when the composites were placed inside the waveguide. It was observed that the higher the % of OPEFB filler, the lower the radiation distribution or the lower is the amplitude of the electric field at the output phase of the waveguide.

References

1. K. E. Dudeck and L. J. Buckley, "Dielectric material measurement of thin samples at millimeter wavelengths," IEEE Transactions on Instrumentation and Measurement, vol. 41, no. 5, pp. 723–725, 1992.View at Publisher · View at Google Scholar · View at Scopus
2. A. Kumar, S. Sharma, and G. Singh, "Measurement of dielectric constant and loss factor of the dielectric material at microwave frequencies," Progress in Electromagnetics Research, vol. 69, PP. 47–54. 2007. View at Google Scholar · View at Scopus
3. James Baker-Jarvis, "Dielectric and magnetic measurement methods in transmission lines: an overview," Proceedings of the 1992 AMTA Workshop, July 25, 1992, Chicago, Illinios.
4. Leo P. Ligthart (1983). "A fast computational technique for accurate permittivity determination using transmission line methods", IEEE Trans. on Microwave Theory and Techniques, Vol. MTT-31, No. 3, pp. 249-254.

5. Dijana, P., Cynthia B., Michal, O., John, H. B, (2005). "Precision open-ended coaxial probes for in-vivo and ex-vivo dielectric spectroscopy of biological tissue at microwaves frequencies". IEEE *Transaction on Microwave Theory and Techniques*, Vol. 53, No.5.
6. Rhodes and Schwarz, (2010). *Measurement of materials dielectric properties*, Application note, R&S.
7. Jin, J. M, (2010). *The Finite Element Method, in Theory and Computation of Electromagnetic Field*, John Wiley & Sons, USA.
8. Barkanov, E. (2001). *Introduction to Finite Element Method, Institute of Materials and Structures*, Riga Technical University, Latvia.
9. C. J. Reddy, et al (1994). "Finite element method for eigenvalue problems in electromagnetic", *NASA Technical Paper* 3485.
10. C. J. Reddy, et al (1995). "Application of FEM to estimate complex permittivity of dielectric material at microwave frequency using waveguide measurements", *NASA Contractor Report*.
11. Pozar, D. M, (2009). *Microwave engineering*, 3rd Edition. John Wiley and Sons Inc. USA.
12. Abbas, Z. Pollard, R. D. and Kelsall, R.W. (2001). Complex Permittivity Measurements at Ka Band Using Rectangular Dielectric Waveguide. *IEEE Transaction on Instrumentation and Measurement*, vol. 50. No. 5, pp 1334-1342.
13. Nicholson, A. M and Ross, G. F, (1970). Measurement of the Intrinsic Properties of Materials by Time Domain Techniques, *IEEE Transaction on Instrumentation and Measurement*, Vol. IM-19, pp 395 – 402.
14. Ramadan, M. A. (2009). Electromagnetic characterisation of Sm-YIG and Sm-YIG-PVDF composites prepared using modified conventional mixing oxide technique [Ph.D. thesis], Universiti Putra, Serdang, Malaysia.
15. Soleimani, H., Yahya, N., Abbas, Z., Soleimani, H., & Zaid, H. M. (2012). Determination Reflection and Transmission Coefficients of Lanthanum Iron Garnet Filled PVDF-Polymer Nanocomposite Using Finite Element Method Modeling at Microwave Frequencies. Journal of Nano Research, 21(January 2016), 151–157. https://doi.org/10.4028/www.scientific.net/JNanoR.21.151
16. Soleimani, H., Yahya, N., Abbas, Z., Soleimani, H., & Zaid, H. M. (2012). Determination Reflection and Transmission Coefficients of Lanthanum Iron Garnet Filled PVDF-Polymer Nanocomposite Using Finite Element Method Modeling at Microwave Frequencies. Journal of Nano Research, 21(January 2016), 151–157. https://doi.org/10.4028/www.scientific.net/JNanoR.21.151.
17. Q. Yuan, D. Wu, J. Gotama, and S. Bateman, J. Thermop. Comp. Mater. 21, 3 (2008).
18. Khalid, M, Ali, S., Abdullahi, C. T. and Choong, S. Y. T. (2006). Effect of MAPP as Coupling Agent on the Mechanical Properties of Palm Fibre Empty Fruit Bunch and Cellulose Polypropylene Biocomposites. International Journal of Engineering and Technology, 3 (1), 79 – 84.

19. Wirjosentono, B., Guritno, P. and Ismail, H. (2004). Oil Palm Empty Fruit Bunch Filled Polypropylene Composites. International Journal of Polymeric Materials 53 (4), 295 – 306.
20. Abu Bakar, A., Hassan, A. and Mohd Yusof, A. F. (2005). Effect of Oil Palm Fruit Bunch and Acrylic Impact Modifer on Mechanical Properties and Processability of Unplasticized Poly(Vinyl Chloride) Composites. Polymer. Plastics Technology andEngineering 44, 1125 – 1137.
21. Rozman, H. D., Tay, G. S. Abubakar, A. & Kumar, R. N. (2001). Tensile properties of oil palm empty fruit bunch-polyurethane composites. European Polymer Journal 37(9), 1759-1765.
22. Rozman, H. D., Ahmadhilmi, K. R. and Abubakar, A. (2004). Polyurethane – Oil palm Empty Fruit Bunch Composites: The Effect of Oil Palm Empty Fruit Bunch Reinforcement on the Mechanical Properties. Polymer Testing 23 (5), 559 – 565.
23. Rozman, H. D., Faiza, M. A. and Kumar, R. N (2008). A Preliminary Study on Ultraviolet Radiation – Cured Biofibre Composites from Oil Palm Empty Fruit Bunch. Polymer Plastics Technology Engineering 47 (4), 358 – 362.
24. Rozman, H. D., Lim, P. P., Abusamah, A., Kumar, R. N., Ismail, H and Mohd Ishak, Z (1999). The Physical Properties of Oil Palm Empty Fruit Bunch Composites made from Various Thermoplastic. International Journal of Polymer Materials 44 (1 & 2), 179 – 195.